Numerical simulation of a rising bubble in viscoelastic fluids

H. Damanik, A. Ouazzi, and S. Turek

Abstract In this paper we discuss simulation techniques for a rising bubble in viscoelastic fluids via numerical methods based on high order FEM. A level set approach based on the work in [9] is used for interface tracking between the bubble and the surrounding fluid. The two matters obey the Newtonian and the Oldroyd-B constitutive law in the case of a viscoelastic fluid while the flow model is given by the Navier-Stokes equations. The total system of equations is discretized in space by the LBB-stable finite element Q_2P_1, and in time by the family of $\theta-$scheme integrators. The solver is based on Newton-multigrid techniques [1, 2] for nonlinear fluids. First, we validate the multiphase flow results with respect to the benchmark results in [4], then we perform numerical simulations of a bubble rising in a viscoelastic fluid and show cusp formation at the trailing edge.

Key words: FEM, viscoelastic, level set method, multiphase flow, cusp shape

1 Introduction

A rising bubble in a viscoelastic fluid shows a different behaviour than in a Newtonian fluid. In the first case, a cusp shape may appear at the trailing edge of the bubble while in the latter, this phenomena does not commonly appear. Thus, it is not only physically interesting but also numerically challenging to simulate such phenomena due to the multiphase characteristics and nonlinearity of the underlying fluid models. As already studied in the viscoelastic benchmark of flow around cylinder [2], the nonzero normal stress difference may exponentially increase behind a stagnation point of the cylinder to balance the almost zero shear rate. Similarly, the same mechanism can be used to describe the negative wake behind the bubble and leads

H. Damanik, A. Ouazzi, S. Turek
Institut fuer Angewandte Mathematik, TU Dortmund, Vogelpothsweg 87 e-mail: hdamanik@mathematik.tu-dortmund.de

to a cusp shape formation [6]. Experimental work has been done in [6] for different types of test liquids, size of the apparatus and volume of the bubbles which leads to a critical non-dimensional capillary number for cusp formation and velocity jump.

The idea to use a numerical approach to reproduce a cusp shape phenomena is not new. There are already methods for solving such complex systems such as lattice Boltzmann [10], finite element [3], finite difference schemes with boundary fitted orthogonal curvilinear coordinate systems [7] which are able to obtain qualitatively experimental results. Basically one needs both Newtonian and viscoelastic fluid models coupled with the well-known Navier-Stokes equations to describe the full domain system. Additionally, there is an interface tracking, resp., capturing algorithm one has to consider. Thus, the complete system of equations is very complex because the interface itself is part of the unknowns. Several tracking algorithms exist in the literature such as volume of fluid, phase field, level set method or coupled level set and volume of fluid [5]. In this study, the level set method of [9] is utilized without special objectivity. In the level set (ϕ) equation, the interface Γ_i between the two immiscible fluids changes its position with time (t) due to convection of the velocity ($\mathbf{u}$) only

$$\frac{\partial \phi}{\partial t} + (\mathbf{u} \cdot \nabla)\phi = 0. \tag{1}$$

The above equation (1) is a pure transport problem which determines the interface of the two (nonlinear) fluids. The good news is that the Newton-multigrid solver together with the high order finite element pair Q_2P_1 has proved successful with respect to such nonlinearity [1,2]. The bad news is that solving the equation changes the property of the level set which should always be a distance function at every time step, that means

$$\|\nabla \phi\| = 1, \ \ \forall \ t \in [0,T]. \tag{2}$$

The standard remedy is re-initialization. A brief overview of types of re-initialization can be seen in [3], see also the work of [8].

The objective of this study is to extend the application of our proposed numerical approach in [2] onto multiphase viscoelastic flow problems. Although a strong coupling of solving the discrete nonlinear system is being focused here, the level set equation is solved separately from the fluid flow model. The viscoelastic flow model is still solved in a fully coupled manner based on the previous work [1,2]. In the next section, we start with the governing equations which then will be followed by the numerical solution technique section. Once we have validated the numerical approach with respect to a benchmark problem for a rising bubble in a Newtonian fluid [4], we describe numerical experiments of a rising bubble in viscoelastic fluids in the next section. We close the article with a summary in the last section.

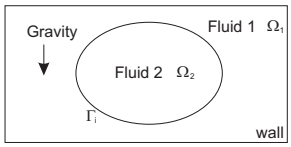

Fig. 1 General setup of two-phase problem with gravity. It shows a bubble placed in another fluid within rectangular geometry.

2 Governing equations

Fluid 1 is a viscoelastic fluid described by the Oldroyd-B model based on the conformation tensor τ (see Fig. 1),

$$\frac{\partial \tau}{\partial t} + \overbrace{(\mathbf{u}\cdot\nabla)\tau}^{\text{convection}} \underbrace{-\nabla\mathbf{u}\cdot\tau - \tau\cdot\nabla\mathbf{u}^T}_{\text{stretching}} + \frac{1}{\Lambda}(\tau - \mathbf{I}) = 0. \tag{3}$$

Fluid 2 is a liquid bubble given by a Newtonian model, $\tau_s = 2\eta_s(\mathbf{x},t)\mathbf{D}$ with constant viscosity $\eta_s(\mathbf{x},t)$ in each fluid phase. Here, $\mathbf{D} = \frac{1}{2}(\nabla\mathbf{u} + \nabla\mathbf{u}^{\mathrm{T}})$ is the deformation tensor. Both fluids are governed by the Navier-Stokes flow equations, i.e.

$$\begin{cases} \rho(\mathbf{x},t)\dfrac{\partial \mathbf{u}}{\partial t} + \rho(\mathbf{x},t)(\mathbf{u}\cdot\nabla)\mathbf{u} = \nabla\cdot\mathbf{T} + \rho(\mathbf{x},t)\mathbf{g} \\ \nabla\cdot\mathbf{u} = 0 \end{cases} \tag{4}$$

where the density depends on the position. The hydrostatic pressure p, the viscous- and the elastic-tensor contribute to the total stress tensor so that we can write

$$\mathbf{T} = -p\mathbf{I} + \tau_s + \frac{\eta_p(\mathbf{x},t)}{\Lambda}(\tau - \mathbf{I}). \tag{5}$$

In Fluid 2 the relaxation time goes to zero, $\Lambda = 0$, which from equation (3) it implies that the conformation stress tensor is equal to unity, $\tau = \mathbf{I}$. This condition defines a stress-less fluid (in the normal direction). Thus the last term of equation (5) cancels out.

As already mentioned, the material properties are constant in each fluid phase. Unfortunately since the interface is unknown one can not a priori set it to Dirichlet data as part of the discrete domain (mesh). Thus material properties change accordingly in particular to the position inside some thickness ε near the interface:

$$\rho(\mathbf{x},t) = \begin{cases} \rho_1, \ \forall\, \mathbf{x} \in \Omega_1(t) \\ \rho_2, \ \forall\, \mathbf{x} \in \Omega_2(t) \\ \rho_2 + \frac{1}{2}\left(1 + \varepsilon + \sin(\pi\varepsilon)/\pi\right)(\rho_1 - \rho_2), \ \forall\, \mathbf{x} \in \Gamma_i \end{cases} . \tag{6}$$

The same rule is applied to the viscosity, $\eta_s(\mathbf{x},t)$ and $\eta_p(\mathbf{x},t)$.

3 Numerical methods

We discretize the above system of equations with second order time integrators such as Crank-Nicolson which belongs to the family of θ-schemes. Given $\mathbf{u}^n$, ϕ^n, τ^n,

$\rho(\mathbf{x},t_n)$, $\eta_s(\mathbf{x},t_n)$, $\eta_p(\mathbf{x},t_n)$ and $\Delta t = t_{n+1} - t_n$, the first numerical step is to seek solutions $\mathbf{u}$, p, τ for the next time step

$$\rho(\mathbf{x},t_n)\frac{\mathbf{u}-\mathbf{u}^n}{\Delta t} + \theta\left[\rho(\mathbf{x},t_n)(\mathbf{u}\cdot\nabla\mathbf{u}-\mathbf{g}) - \eta_s(\mathbf{x},t_n)\Delta\mathbf{u} - \frac{\eta_p(\mathbf{x},t_n)}{\Lambda}\nabla\cdot\tau\right] + \nabla p$$

$$+(1-\theta)\left[\rho(\mathbf{x},t_n)(\mathbf{u}^n\cdot\nabla\mathbf{u}^n-\mathbf{g}) - \eta_s(\mathbf{x},t_n)\Delta\mathbf{u}^n - \frac{\eta_p(\mathbf{x},t_n)}{\Lambda}\nabla\cdot\tau^n\right] = 0 \quad (7)$$

$$\nabla\cdot\mathbf{u} = 0 \quad (8)$$

where $\mathbf{u}^n \sim \mathbf{u}(t_n)$. As one can see, the pressure space is discretized fully implicitly. The Oldroyd-B model is discretized simultaneously in the same way so that

$$\frac{\tau-\tau^n}{\Delta t} + \theta\left[\mathbf{u}\cdot\nabla\tau - \nabla\mathbf{u}\cdot\tau - \tau.\nabla\mathbf{u}^T + \frac{1}{\Lambda}(\tau-\mathbf{I})\right]$$

$$+(1-\theta)\left[\mathbf{u}^n\cdot\nabla\tau^n - \nabla\mathbf{u}^n.\tau^n - \tau^n.\nabla\mathbf{u}^n + \frac{1}{\Lambda}(\tau^n-\mathbf{I})\right] = 0. \quad (9)$$

This maintains the monolithic character of solving and the accuracy of the solutions vector for the next numerical step. The second numerical step reads: Given $\phi^n, \mathbf{u}$, we seek solutions for the next time step of the level set equation

$$\frac{\phi-\phi^n}{\Delta t} + \theta\left[\mathbf{u}\cdot\nabla\phi\right] + (1-\theta)\left[\mathbf{u}\cdot\nabla\phi^n\right] = 0. \quad (10)$$

This step is exclusively decoupled from the first numerical step so that one can directly apply, if needed, standard numerical ingredients to stabilize the solver. In this step we observe that the high order finite element does not need numerical stabilization, but may not maintain mass conservation.

In each time step, the problem is discretized in space with the high order finite elements $Q_2P_1/Q_2/Q_2$ for velocity-pressure, (elastic) stress and level set.

The third numerical step is the re-initialization of ϕ. We recalculate the function value, to be almost exact, which is referred as "brute force", after finding all zero function values (interface). Thus, the accuracy depends on the number of interface points found on the finite element being used (see Fig. 2).

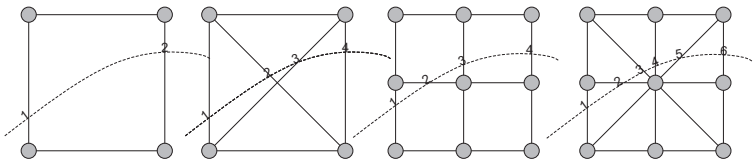

Fig. 2 Different possibilities of finding interface points in a finite element.

4 Surface tension

The surface tension of a liquid in real problem can not be neglected. One can consider it as additional volume force, $\mathbf{F}_{st}$, applied to the flow equation (4)

$$\mathbf{F}_{st} = \sigma\kappa\mathbf{n}. \tag{11}$$

The calculation of this force needs not only the gradient of level set $\mathbf{n}$ but also the curvature κ

$$\mathbf{n} = \nabla\phi, \quad \kappa = -\nabla\cdot\mathbf{n}. \tag{12}$$

While the gradient of the level set is provided within the finite element space, the curvature needs extra calculation after the third numerical step. One way to get this curvature is by projecting it into the finite element space $\tilde{\kappa} \in Q_2$ by solving

$$\int_\Omega \tilde{\kappa}\psi = -\int_\Omega (\nabla\cdot\mathbf{n})\psi \quad \forall\psi \in Q_2. \tag{13}$$

5 Rising bubble benchmark

5.1 Rising bubble benchmark in Newtonian fluids

The classical benchmark of rising bubble is taken into account, please look at the webpage http://www.featflow.de/en/benchmarks/cfdbenchmarking/bubble.html. We consider only test case 1 as comparison. A bubble is placed at the lower part of a 1×2 rectangular geometry with a radius of $r = 0.25$. Given a different density and viscosity between the two immiscible fluids, the bubble rises due to buoyancy force when solving the Navier-Stokes equations. Quantitative data measurements are undertaken in post-processing calculation, namely the center point of the bubble $\mathbf{X}_c = (x_c, y_c)$, the rising velocity $\mathbf{U}_c$ and the circularity ϕ of the bubble shape

$$\mathbf{X}_c = \frac{\int_{\Omega_2}\mathbf{x}\,dx}{\int_{\Omega_2}1\,dx}, \quad \phi = \frac{\pi d_a}{P_b}, \quad \mathbf{U}_c = \frac{\int_{\Omega_2}\mathbf{u}\,dx}{\int_{\Omega_2}1\,dx}. \tag{14}$$

The way to integrate these functional values may use the finite element function in each cubature point. A function value is included in the integration if the corresponding cubature point lies within the bubble domain Ω_2. In this way, it is efficient but it may not give accurate solution data. A more accurate way is to take the sum of all area of triangles and rectangles respectively within Ω_2. Details of boundary conditions can be also seen in the above mentioned website.

5.2 Rising bubble in viscoelastic fluids

There is no rigorous benchmark for a rising bubble in a viscoelastic liquid, but there exist numerical simulations for this purpose which tried to show cusp shape as observed in the experimental results. There are 2 types of simulations in literature: i) A constant velocity data is given at the top boundary and then by buoyancy force the bubble remains still while a steady shape of the bubble can be obtained with marching of the time, see for example [7] and ii) No velocity data is imposed and by buoyancy force the bubble rises and deforms its shape with time, i.e. [10]. Either way, the objective of the simulation is to obtain the cusp shape of the bubble. In this study we follow the second setup.

6 Numerical results

6.1 Rising bubble in Newtonian fluids

The plots of circularity, center point, rising speed and the bubble shape are given in Fig. 3 which correspond to test case 1 in [4]. The high order finite element competes very fine with the ones from the benchmark that use low order FEM. The circularity of the bubble differs slightly at time $t = 3$. This can be due to no special treatment for mass loss when solving for the level set, while in the benchmark, artificial mass conservation as well as FEM-TVD stabilization has been used (by Group 1). However, the center point plot agrees very well with the reference data. The rising speed

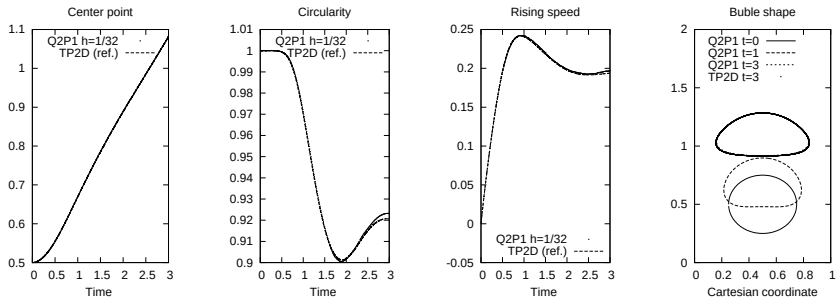

Fig. 3 Circularity and center point of the bubble the against benchmark data in [4].

of the bubble agrees very well, too. Although the shape looses slightly mass at time $t = 3$, it can be accepted for the coarse mesh being used. We consider that our results are quite accurate with respect to the benchmark and continue with a rising bubble in viscoelastic fluids.

6.2 Rising bubble in viscoelastic fluids

The cusp formation is subject to certain conditions: The inertia effect (Re) must be small but the rising speed should be visible, the capillary number (Ca) should be bigger than some critical number and the Weissenberg number does not vanish (We $\neq 0$) [6]. Therefore the parameter setting from the previous benchmark is not suitable here. We re-set the parameter setting to be as in the following tabular to obtain different bubbles formation.

Test case	ρ_1	ρ_2	η_1	η_2	$\mathbf{g}$	σ
1. Viscoelastic ($\Lambda = 10$)	10	0.1	10	1	9.8	0.245
2. Newtonian ($\Lambda = 0$)	10	0.1	10	1	9.8	0.245
3. Viscoelastic ($\Lambda = 10$)	10	0.1	2	1	9.8	0.245
4. Newtonian ($\Lambda = 0$)	10	0.1	2	1	9.8	0.245

On the other hand the geometrical configuration is kept the same as in the previous benchmark because the shape of the column does not influence the cusp formation [6] as long as it is aligned with the gravity (the column does not tilt). The first two test cases (Fig. 4) show a different rising bubble behaviour in viscoelastic and Newtonian surrounding fluids. The cusp starts to appear very late at numerical time $t = 5$. On the other hand, the last two test cases (Fig. 4) show that the bubble rises

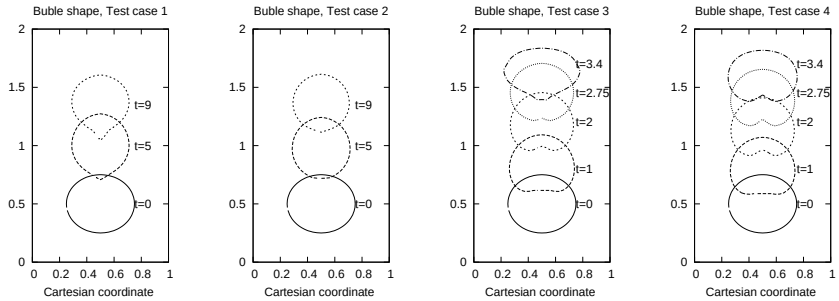

Fig. 4 Evolution of bubbles of test cases 1-4

faster than the first two test cases because of more inertia. Already at time $t = 3.4$ the bubble is close to the upper wall which shows cusp formation. Since the numerical time is shorter than the first two test cases, mass loss is less visible here.

7 Summary

We have analyzed numerical test cases that show cusp shape formation of a bubble when rising in viscoelastic fluids. A high order finite element approach is utilized for discretizing both fluid domains as well as the interface. The solver for the viscoelastic fluids is treated in a monolithic approach while the level set equation is solved separately from the fluid part. The numerical results are validated for a rising bubble in a Newtonian fluid which can be considered as quite accurate. Anyway, mass loss of the bubble is still present for the level set method with the chosen re-initialization. Further work is in progress in such a way that re-initialization does not introduce mass loss.

Acknowledgement The authors would like to thank the German Reasearch Foundation (DFG) for supporting the work through collaborative research center SFB/TR TRR 30.

References

1. Damanik, H., Hron, J., Ouazzi, A., Turek, S.: A monolithic FEM–multigrid solver for non-isothermal incompressible flow on general meshes. Journal of Computational Physics **228**, 3869–3881 (2009)
2. Damanik, H., Hron, J., Ouazzi, A., Turek, S.: A monolithic FEM approach for the log-conformation reformulation (lcr) of viscoelastic flow problems. Journal of Non-Newtonian Fluid Mechanics **165**, 1105–1113 (2010)
3. Hysing, S.: Numerical simulation of immiscible fluids with FEM level set techniques. Ph.D. thesis, Technische Universität Dortmund (2007)
4. Hysing, S., Turek, S., Kuzmin, D., Parolini, N., Burman, E., Ganesan, S., Tobiska, L.: Quantitative benchmark computations of two-dimensional bubble dynamics. International Journal for Numerical Methods in Fluids **60 Issue 11**, 1259–1288 (2009)
5. Jimenez, E., Sussman, M., Otha, M.: A computational study of bubble motion in newtonian and viscoelastic fluids. Fluid Dynamics and Material Processing 1 **2**, 97–108 (2005)
6. Liu, Y. J., Liao, T. Y., Joseph, D. D.: A two-dimensional cusp at the trailing edge of an air buble rising in a viscoelastic liquid. Journal of Fluid Mechanics **304**, 321–342 (1995)
7. Noh, D. S., Kang, I. S., Leal, L. G.: Numerical solutions for the deformation of a buble rising in dilute polymeric fluids. Physics of Fluids **5**, 1315–1332 (1993)
8. Olsson, E., Kreiss, G.: A conservative level set method for two phase flow. Journal of Computational Physics **210**, 225–246 (2005)
9. Sethian, J.: Level Set Methods and Fast Marching Methods: Evolving Interfaces in Computational Geometry, Fluid Mechanics, Computer Vision, and Material Science. Cambridge University Press (1999). 2nd edition
10. Yoshino, M., Toriumi, Y., Arai, M.: Lattice boltzmann simulation of two-phase viscoelastic fluid flows. Journal of Computational Science and Technology **2**, 330–340 (2008)